

Numerical Analysis of Bubble Powered Micropump

G. A. Pinhasi¹, M. Pe'er^{1,2,3} and A. Ullmann²

1. Dept. of Chemical Engineering, Ariel University., ISRAEL
2. School of Mechanical Engineering, Tel Aviv University, ISRAEL
3. Israel Aerospace Industries, IAI, ISRAEL

Introduction

Development of micro-pumps will allow the minimization of many mechanical, bio-engineered and electrical systems, for example: controlled drug delivery systems or liquid cooled microprocessors. The development of such system is facing two major challenges: the design of actuation mechanism and the flow direction control.

Many design concepts and prototype micro-pumps have been demonstrated over the past decade, such as: mechanical displacement, bubble, electro-hydrodynamic, and electro-capillary. For the flow direction control there is a use of micro valves or valve-less micro-pump by means of nozzle-diffuser design. In order to design high performances systems a modeling study must be performed.

In the present work a numerical model was developed to simulate the operation of a micro-pump driven by bubble formation and growth after Tsai and Lin (2002) design^{1,2} (Figure 5). For such a design, only relatively simple lumped parameter model was suggested³. The present model consists of a full description of bubble formation and growth mechanisms.

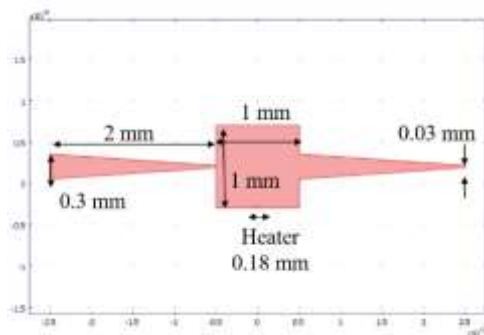


Figure 1: Bubble Pump Geometry

Theory

The thermal-bubble-actuated micropump is a "no moving parts" design creating an unsteady pumping liquid flow. The micropump is using the principles of liquid/vapor phase transition and nozzle-diffuser flow direction control. The micropump consists of a pumping chamber, a pair of nozzle-diffuser flow controllers and a resistive heater.

The actuation mechanism comes from periodically nucleating and collapsing thermal bubbles. A net flow is generated from the nozzle to the diffuser by the nozzle-diffuser flow controller.

The bubble pump actuation can be divided into stages: first the liquid is heated until critical saturation conditions for bubble formation are achieved. Following, the bubble grows and pushes the liquid from the pumping chamber toward the nozzle-diffuser system. After the heating stops, the bubble collapse and new liquid enters the pumping chamber.

The Model

The model solves the time dependent conservation equation for viscous fluid: mass, momentum and convection heat transfer. The Level-Set method is being used, to represent the gas-liquid interface.

The analysis is made by using finite element software COMSOL Multiphysics, the model code was written and activated using MATLAB environment. Fluid Mechanics and Heat Transfer modules were used with the steam tables for water properties. The different stages were synchronized and controlled with the MATLAB code.

1. Conservation Equations

Continuity

$$\frac{\partial \rho}{\partial t} + \nabla \circ (\rho \mathbf{u}) = 0 \quad (1)$$

Momentum (Navier-Stokes, NS)

$$\begin{aligned} \rho \left[\frac{\partial \mathbf{u}}{\partial t} + (\mathbf{u} \circ \nabla) \mathbf{u} \right] = \\ = \rho \mathbf{g} - \nabla P + \sigma \kappa \delta \mathbf{n} + \\ + \nabla \circ \left\{ \mu \left[\nabla \mathbf{u} + (\nabla \mathbf{u})^T - \frac{2}{3} (\nabla \circ \mathbf{u}) \mathbf{I} \right] \right\} \end{aligned} \quad (2)$$

Energy: Convective Heat transfer

$$\begin{aligned} \rho C_p \left(\frac{\partial T}{\partial t} + \mathbf{u} \circ \nabla T \right) = \\ = \nabla \circ (k \nabla T) - \dot{m}'' h_{LG} \delta \end{aligned} \quad (3)$$

where $\mathbf{u}(\mathbf{x}, t)$ is the velocity vector $\rho(\mathbf{x}, t)$ is the fluid density (vapor and liquid), $T(\mathbf{x}, t)$ is the temperature, $P(\mathbf{x}, t)$ is the pressure. The fluid properties are: μ viscosity, σ surface tension, k thermal conductivity, C_p specific heat capacity, h_{fg} heat of evaporation. The interface geometry defied by: \mathbf{n} the normal vector and κ the curvature.

Heat and Mass relation at the interface

$$\dot{m}_i'' = \frac{k \nabla T \circ \mathbf{n}}{h_{LG}} \quad (4)$$

where \dot{m}_i'' is the mass flux evaporation rate.

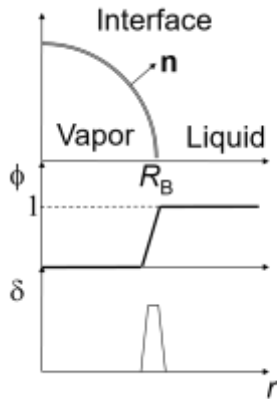


Figure 2: The interface and the level-set parameters

Level-Set

$$\begin{aligned} \frac{\partial \phi}{\partial t} + \mathbf{u} \circ \nabla \phi + \frac{\dot{m}_i''}{\rho} |\nabla \phi| = \\ = \gamma \nabla \circ \left[\varepsilon \nabla \phi - \phi (1 - \phi) \frac{\nabla \phi}{|\nabla \phi|} \right] \end{aligned} \quad (5)$$

where $\phi(\mathbf{x}, t)$ is the level-set parameter ($\phi=0$ vapor; $\phi=1$ Liquid), δ is the delta function ($\delta(\mathbf{x}, t) = 6 |\nabla \phi| |\phi(1-\phi)|$), γ and ε are constants (Figure 2).

The fluid properties at any point is found using the "lever rule" and the level-set parameter/ for example, the density is calculated using

$$\rho = \rho_G + (\rho_L - \rho_G) \phi \quad (6)$$

The interface velocity is

$$\mathbf{u}_{\text{interface}} = \mathbf{u} + \frac{\dot{m}_i''}{\rho} \mathbf{n} \quad (7)$$

and its normal

$$\mathbf{n} = \frac{\nabla \phi}{|\nabla \phi|} \Big|_{\phi=0.5} \quad (8)$$

2. Bubble Life Cycle

During a single pumping cycle, the bubble passes four stages in its life cycle. The pump performance is determined by cycle time and heater duty cycle.

a. Initial liquid heating

The heater is turned on to heat the liquid up to its boiling point. The model solves a conduction / force convection problem to calculate the temperature map near the heater.

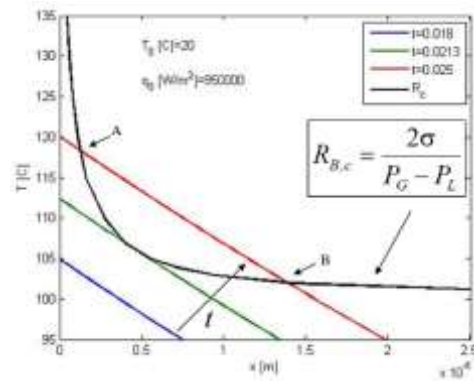


Figure 3: Nozzle-Diffuser: Pressure profile

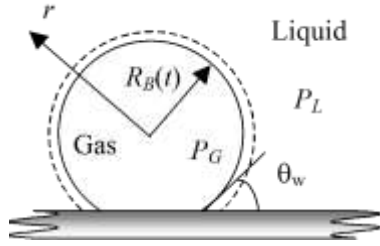


Figure 4: Bubble growth on a wall

b. Formation of a critical bubble

The bubble growth from an incipient nucleation site would begin when temperature of the fluid around a hemispherical bubble exceeds the equilibrium temperature of a stable bubble of the same radius (Figure 3)⁴.

Thus a criterion for the wall nucleation can be found, considering the thermal boundary development and the critical bubble size models together (Hsu's criterion). The intersection of the temperature profile and critical bubble size curves yields the location of the smallest stable vapor embryo which can be formed.

c. Bubble growth

After defining the initial bubble size and shape from the bubble formation sub-model, the initial bubble vapor domain (any point above the boiling temperature) and its interface are set using geometry tool.

As the two phase (Liquid-vapor) interface is set, the conservation equations including the level set equation are being solved to find the flow field in the pump system (Figure 4)⁴.

d. Bubble Collapse

When the heater is turned off, the bubble starts shrinking due to heat loss to the cold liquid away from the bubble. As the bubble reaches its critical size, the vapor domain is being canceled. The system returns to stage (a) with single liquid phase. The critical bubble size is being calculated due to the criterion presented in stage (b).

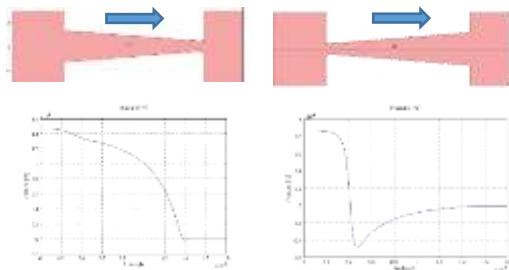


Figure 5: Nozzle-Diffuser: Pressure profile: Flow direction right to left

Simulation Results

Each sub-model was separately evaluated with literature results: nozzle-diffuser flow characteristics, nozzle-diffuser displacement driven pump, spherical homogeneous bubble growth and finally bubble driven micro- pump.

1. Nozzle-Diffuser Operation

The nozzle-diffuser steady state flow losses were studied to find the net flow rate through the system. The pressure profile for the nozzle and the diffuser are presented in Figure 5.

For the nozzle-diffuser, the minor losses coefficient ξ , is defined as

$$\Delta P = \xi \frac{1}{2} \rho \bar{u}_{throat}^2 \quad (9)$$

where ΔP is the pressure gradient. The steady state minor losses coefficient for each device as a function of Reynolds number is presented in Figure 6, for Jung and Kwak (2007) geometry². It seems that for laminar flow minor losses coefficient difference between the nozzle and diffuser is increased.

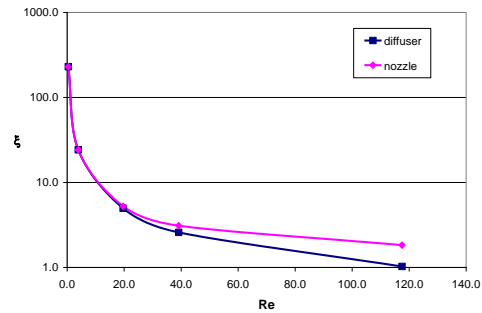


Figure 6: Minor losses coefficient: nozzle/diffuser

2. Bubble Pump

In the present paper 2D bubble pump results are presented. The model was implemented for test cases with heating flux range of $900 \div 1000 \text{ kW/m}^2$ (Heater length 0.18mm).

In Figure 7 the pump system and the pressure map is presented. During the bubble growth the pressure in the pumping chamber is high compared to the inlet-outlet channels.

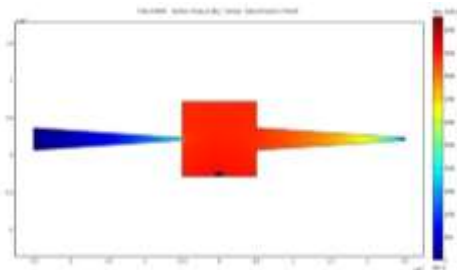


Figure 7: Pump pressure map ($t=0.0253s$)

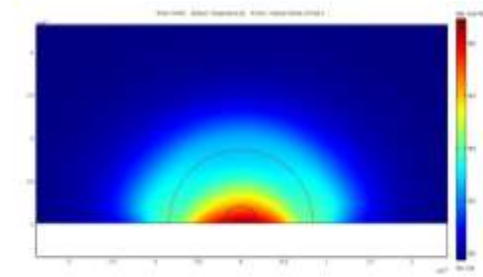


Figure 8: Pump Characteristics (Flow-rate, Head)

3. Heating and Bubble boundary

At the heating stage, the heater is on and the heated liquid reaches the boiling conditions. The temperature map prior to the bubble formation is presented in Figure 8.

4. Bubble size history

Bubble life cycle during a single pumping cycle is presented in Figure 9. The heat flux is 1000 kW/m^2 (33 Hz) with 80% duty cycle. From the bubble radius time history, one can see the relatively long incubation time and the short bubble action time. The net flow rate in this case was $9.14 \text{ } \mu\text{l/min}$

5. Pump Characteristics

The pump flow characteristics, the flow rate Q , the head, h_p and the efficiency η , were obtained by averaging the flow properties with respect to time:

$$\bar{Q}_{net} = \frac{1}{T_{cycle}} \int_0^{T_{cycle}} (Q_{b1} - Q_{b2}) dt \quad (10)$$

$$\Delta P = \frac{1}{T_{cycle}} \int_0^{T_{cycle}} (P_{b1} - P_{b2}) dt$$

$$\eta = \frac{\int_0^{T_{cycle}} (Q_{b1} - Q_{b2}) \Delta P dt}{\int_0^{T_{cycle}} q dt}$$

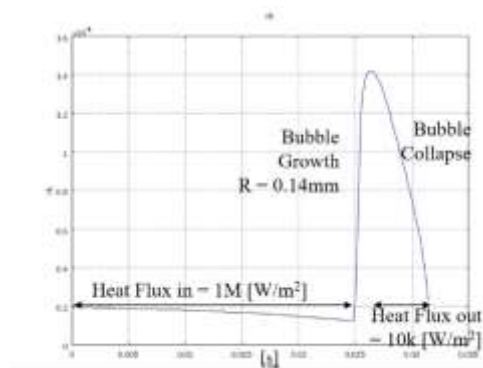


Figure 9: Bubble size history- Single cycle

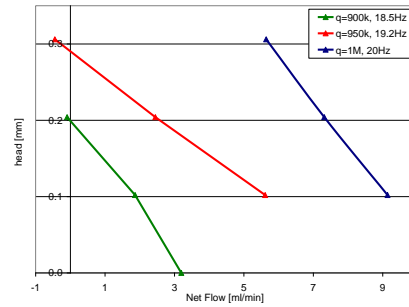


Figure 10: Pump Characteristics (Flow-rate, Head)

The model was applied to find the flowrate-head relations, for different heat flux values: $q'' = 900 \text{ kW/m}^2$ (29 Hz), 950 kW/m^2 (31 Hz) and 1000 kW/m^2 (33 Hz).

The pump characteristics is presented in Figure 10. The obtained Flow rate and the head ranges are $0 \div 9.14 \text{ } \mu\text{l/min}$, $0 \div 0.3 \text{ mm}$. As expected the flow rate decreases as the head increases.

Conclusions

A numerical model was developed to simulate the operation of a micro-pump driven by bubble formation and growth. In the current stage in this study the model is extended for 3D case multi cycle simulation.

References

1. Tsai, J.H. Lin, L. (2002) "A thermal-bubble-actuated micronozzle-diffuser pump", *J. Microelectromech. Syst.*, 11, 665-671.
2. Jung, J.Y. and Kwak, H.Y (2007) "Fabrication testing of bubble powered micropumps using embedded microheater", *J. Microfluid Nanofluid*, 3, 161-169.
3. Qu, Y. and Zhou, J. (2017) "Lumped parameter model and numerical model of vapor bubble-driven valve-less micro-pump", *Advances in Mechanical Engineering*, 9(4) 1-7.
4. Pinhasi, G.A., Dayan, A. and Ullmann, (2005) "Modeling of Flashing Two-Phase Flow", *Reviews in Chemical Engineering*, 21(3-4), 133-264.